# Last stage control and mechanical transfer function measurement of the VIRGO suspensions

A. Bozzi, C. Bourgoin, S. Cortese, A. Errico, D. Enard, S. Mataguez, A. Paoli, A. Pasqualetti, P. Popolizio, F. Richard, J. M. Teuler, and Z. Zhang
*EGO, Traversa H di via Macerata, 56021, S. Stefano a Macerata (Pi), Italy*

C. Boccara, M. Leliboux, V. Loriette, V. Reita, and J. P. Roger
*ESPCI, 10 Rue Vauquelin, 75005 Paris, France*

P. Ganau, B. Lagrange, J. M. Mackowski, C. Michel, J. L. Montorio, N. Morgado, L. Pinard, and A. Remillieux
*IPNL, 43 Boulevard du 14 Novembre 1918, 69622 Villeurbanne Cedex, Lyon, France*

L. Bracci, G. Calamai, E. Cuoco, P. Dominici, L. Fabbroni, G. Guidi, G. Losurdo, F. Martelli, M. Mazzoni, M. Ripepe, R. Stanga, and F. Vetrano
*Istituto Nazionale di Fisica Nucleare, Sez. Firenze, Largo E. Fermi 2, 50125 Firenze, Italy*

F. Acernese, F. Barone, E. Calloni, S. Cavaliere, M. De Rosa, R. De Rosa, L. Di Fiore,[a] A. Eleuteri, G. Evangelista, F. Garufi, M. Maiorino, L. Milano, K. Qipiani, S. Solimeno, and M. Varella
*Istituto Nazionale di Fisica Nucleare, sez. Napoli, and Dipartimento di Scienze Fisiche, University of Napoli "Federico II," Complesso Universitario di Monte S. Angelo, Via Cintia 80126 Napoli, Italy Dipartimento di Scienze Farmaceutiche, University of Salerno, Via Ponte Don Melillo, 84084 Fisciano (Sa) Italy*

P. Amico, C. Cattuto, L. Gammaitoni, F. Marchesoni, M. Punturo, and H. Vocca
*Istituto Nazionale di Fisica Nucleare, sez. Perugia and University of Perugia, Via A. Pascoli 06123, Perugia, Italy*

G. Ballardin, S. Braccini, C. Bradaschia, C. Casciano, R. Cavalieri, R. Cecchi, G. Cella, V. Dattilo, A. Di Virgilio, I. Ferrante, F. Fidecaro, F. Frasconi, G. Gennaro, A. Giazotto, L. Holloway, P. La Penna, T. Lomtadze, L. Nicolosi, F. Paoletti, R. Passaquieti, D. Passuello, R. Poggiani, R. Taddei, and A. Vicere
*Istituto Nazionale di Fisica Nucleare, Sez. Pisa, Via Livornese 1291, 56010 S. Piero A Grado (Pi), Italy*

S. Frasca, E. Majorana, C. Palomba, M. Perciballi, P. Puppo, P. Rapagnani, and F. Ricci
*Istituto Nazionale di Fisica Nucleare, Sez. Roma I, Piazzale Aldo Moro 5, 00185 Roma, Italy*

N. Arnaud, C. Arnault, M. Barsuglia, J. L. Beney, R. Bilhaut, M. A. Bizouard, V. Brisson, P. Canitrot, F. Cavalier, R. Chiche, S. Cuzon, M. Davier, M. Dehamme, C. Eder, M. Gaspard, P. Hello, P. Heusse, E. Jules, O. Lodygenski, B. Mansoux, J. C. Marrucho, M. Mencik, P. Marin, T. Pradier, A. Reboux, P. Rivoirard, and M. Taurigna
*Laboratoire de l'Accelerateur Lineaire, B.P. 34, 91898, Orsay, Fance*

F. Bellachia, D. Boget, D. Buskulic, B. Caron, F. Chollet, P. Y. David, D. Dufournaud, R. Flaminio, L. Fournier, L. Giacobone, C. Girard, R. Hermel, J. C. Lacotte, B. Lieunard, F. Marion, A. Masserot, L. Massonnet, B. Mours, P. Mugnier, J. Ramonet, R. Sottile, D. Verkindt, O. Veziant, and M. Yvert
*LAPP, Chemin de Bellevue, B.P 110, 74941, Annecy-le Vieux Cedex, France*

D. Babusci, H. Fang, G. Giordano, M. Iannarelli, and E. Turri
*INFN Laboratori Nazionali di Frascati, Via E. Fermi 40, 00044 Frascati (Roma), Italy*

F. Bondu, A. Brillet, J. Cachenaut, F. Cleva, T. Cokelaer, J. P. Coulon, J. D. Fournier, H. Heitmann, J. M. Innocent, M. Loupias, C. N. Man, J. Pacheco, T. Regimbau, J. P. Scheidecker, H. Trinquet, P. Tourrenc, and J. Y. Vinet
*Observatoire de la Cote d'Azur, B.P. 4229, 06034, Nice Cedex 4, France*

(Received 2 November 2001; accepted for publication 10 December 2001)

 

The automatic control of the suspended mirrors is a major task in operating an interferometric gravitational wave antenna. To reach the extreme sensitivity required for this kind of detector, an accurate alignment and a stable locking of the interferometer on its working point are crucial. The solution of this problem is particularly complex in the case of a multistage pendulum, such as the suspension system for seismic isolation adopted in VIRGO. A precise knowledge of the suspension mechanical transfer functions (TFs) for different forces applied in the control servo-loops represents essential information to reach the goal. In this article, we describe the apparatus we developed to measure the VIRGO suspension TF and we report the results thus obtained on full-scale suspensions at the VIRGO site. Preliminary results for the implemented control system of the last suspension stage are also presented.  [DOI: 10.1063/1.1463717]

## I. INTRODUCTION

Ground based interferomeric gravitational wave (GW) detectors[1] are long base line Michelson interferometers (MIs) whose arms host long Fabry–Perot (FP) cavities or optical delay lines. The typical arm length ranges from a few hundred meters[2,3] to a few km.[4,5] To reach the extreme sensitivity required for GW detection, all the optical components of such a detector must be carefully isolated from all the sources of external disturbance. In particular, in order to filter ground vibrations, the mirrors are suspended to seismic attenuators, which are essentially pendula, for horizontal isolation, but with an adequate elastic internal structure for vertical isolation. Such an attenuator gives a good attenuation of seismic oscillations at frequencies above its pendulum normal modes (NMs), the drawback being that, at the NM frequencies, the mirrors can undergo rather large oscillations (up to several hundred microns). For this reason, an automatic control system is necessary to damp the NM oscillations and to control the relative orientation and position of the mirrors in order to align the interferometer and lock it on the working point (dark fringe for the MI and resonance for the FP cavities). The error signals for the servomechanism, which operates on many degrees of freedom (DOF) are provided by the interferometer itself and by additional local measurement systems (position sensors, accelerometers). The actuators are generally coil/magnet pairs; by regulating the current flowing in the coils it is possible to exert forces on magnets that are placed at different positions on the suspension and then to induce translations or rotations to the suspended optical components [mirrors, beam splitter (BS), etc.].

For the VIRGO interferometer, the suspension is a multistage seismic isolator, called superattenuator (SA), made of a preisolation stage (an inverted pendulum supporting the top stage of the suspension), a cascade of five passive isolation stages, and a lower part with a steering element, called ''marionetta,'' to which the test mass of the suspension (that is one of the optical elements of the interferometer) and a recoil mass, called ''reference mass,'' are suspended. A detailed description of the SA can be found in Ref. 6. The SA permits to extend the VIRGO frequency band for GW detection down to about 4 Hz; the price to pay is the extreme complexity of the mechanical behavior of the suspension.

To control the test mass movement, forces can be applied on the SA at various levels. There are three coils, attached to the external structure surrounding the SA, acting on the top stage (used for inertial damping[7] and dc control). Four coils (two horizontal and two vertical) are mounted on legs attached to the last passive filter (called ''filter 7'' for historical reasons) and act on four magnets glued to the arms of the marionetta; these coils allow to apply a force on the marionetta center of mass in the direction of the interferometer optical axis and torques around axes orthogonal to the (interferometer) optical axis. Four more (horizontal) coils are attached to the reference mass acting on four magnets directly attached to the back surface of the test mass. Further information on the actuators acting on the SA can be found in Ref. 8.

In order to design the complex servo-loops[9,10] required to control the SA of the VIRGO antenna, accurate knowledge of the mechanical TF is necessary; to this purpose, a dedicated interferometric device was designed which allowed a noncontact TF measurement by sending a laser beam on the surface of the optical element and looking at the reflected beam. In a previous article,[11] we describe in detail the motivation and the principles of operation of such a device and report on preliminary testing performed on a prototype. A new version of the earlier device has been designed in order to measure the TF of the final SA at the VIRGO site in Cascina, based on the same principle of operation but with a completely different optical layout, compatible with the detector geometry. In this article we describe in detail this device and report the actual measurements performed on two of the VIRGO suspensions. In particular they are the BS suspension and the one of the input mirrors of the west arm of the interferometer WI. The measured TFs have been used to design the servo-loops to control the mirror position with respect to a local reference provided by the measurement device itself; preliminary results are reported in a dedicated section.

## II. INSTRUMENT DESCRIPTION

In Fig. 1, we show the schematic setup for TF measurement. A laser beam is sent through an optical window to the surface of the optical component that is suspended under vacuum. The reflected beam exits the vacuum tank through a second window, is reflected by a mirror back to the test mass surface, and then is further reflected to the entrance window.

[a]Author to whom correspondence should be addressed; electronic mail: luciano.difiore@na.infn.it

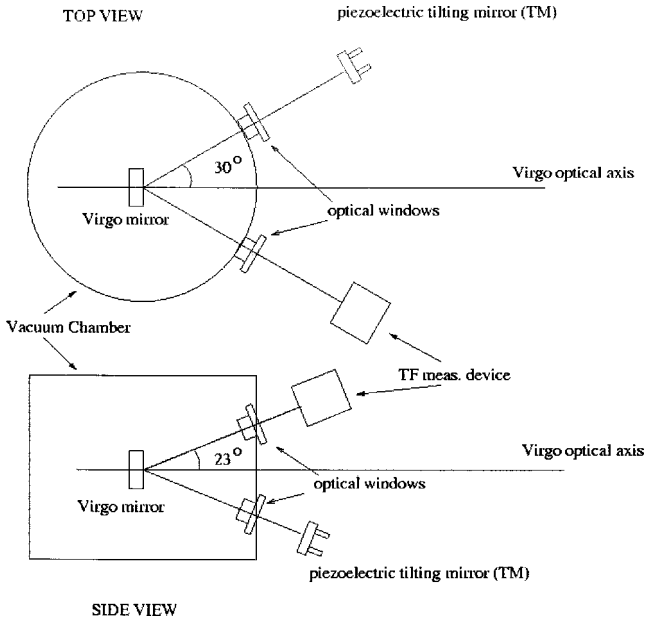


FIG. 1. Schematic setup for TF measurement.

The movement of the suspended mirror can be measured by looking at the reflected beam (assuming that the displacements of the test mass are larger that those of the other elements of the apparatus). In particular, we are interested in three DOF of the suspended mirror, namely the displacement $Z$ along the optical axis (orthogonal to the mirror surface) and the rotations ($\theta_x$ and $\theta_y$) around axes orthogonal to the optical axis (pitch and yaw, respectively).

The displacement $Z$ is measured by a Mach–Zehnder interferometer; one of the two arms is the beam reflected by the suspended mirror, while the other (reference arm) is folded several times on a rigid platform. The angular measurement is provided by a position sensing device (PSD) illuminated by a small fraction of the reflected beam and mounted on the same rigid platform.

In Fig. 2 we sketched the optical setup. The main difference with respect to the setup described in Ref. 11 is that a large part of the optical path is in fiber optics. This is mainly

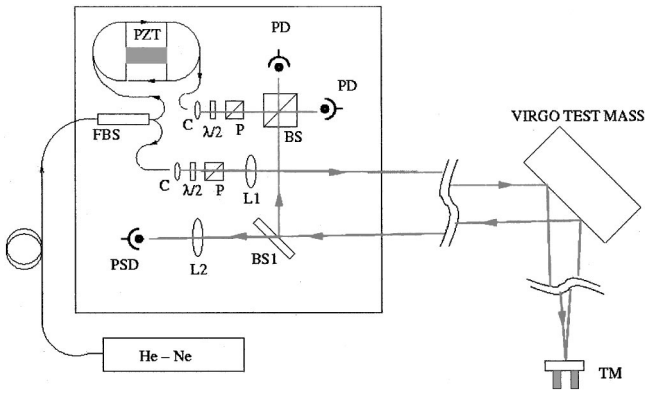


FIG. 2. Optical scheme for TF measurement. FBS = fiber beam splitter, $C$ = fiber output coupler, $\lambda/2$ = half-wave plate, $P$ = polarizer, PZT = piezoelectric fiber stretcher, BS = beam splitter, $L1 = 15$ cm focal length lens, BS1 beam sampler, PD photodiode, $L2 = 10$ cm focal length lens, PSD = position sensing device, TM = piezoelectric tilting mirror.

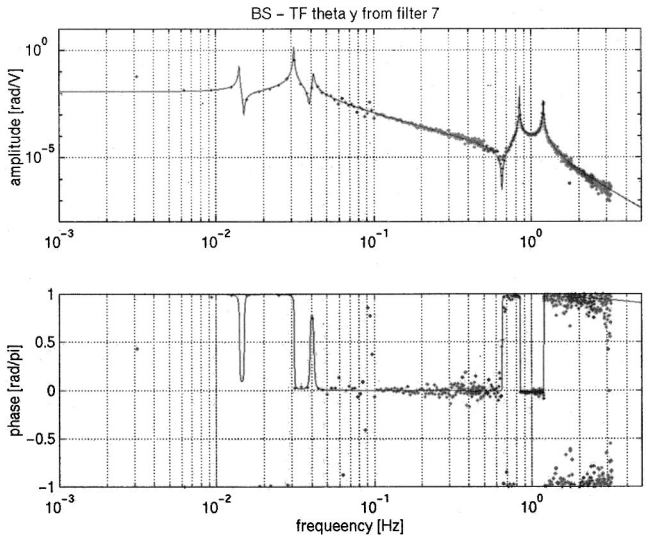


FIG. 3. BS suspension; $\theta y$ (yaw) transfer function for a torque applied on the marionetta with the two horizontal coils of the filter 7 (points) compared with an analytical curve fitted to the data (solid line).

necessary to reduce the overall size of the detector so as to fit the limited space available around the VIRGO vacuum chambers. A second important point is that, due to the position of the optical windows on the vacuum tanks, the optical beam plane is not horizontal, but its normal is at an angle of about 23° with the normal (Fig. 1).

The light source is a single-mode He–Ne laser that lights the device through a single mode optical fiber. On the first platform there is a fiber beam splitter FBS that is the input BS of the Mach–Zehnder interferometer. At the exit of the FBS, one of the two fiber arms, that is, the reference arm of the interferometer, is folded several times on a home-made piezoelectric fiber stretcher (PZT) which is used as an actuator to control the optical path length (OPL) and then to hold the interferometer locked on the fringe, and for calibration. At the end of the fiber there is an output coupler and some polarization control optics (a half-wave plate and a polariz-

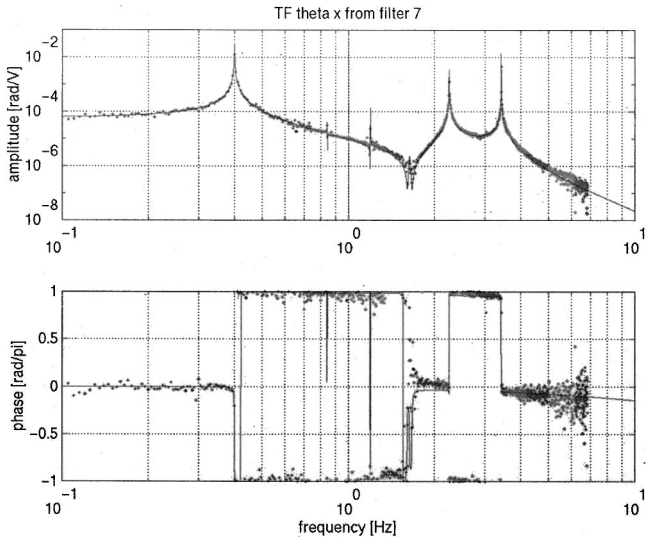


FIG. 4. BS suspension; $\theta x$ (pitch) transfer function for a torque applied on the marionetta with the two vertical coils of the filter 7 (points) compared with an analytical curve fitted to the data (solid line).

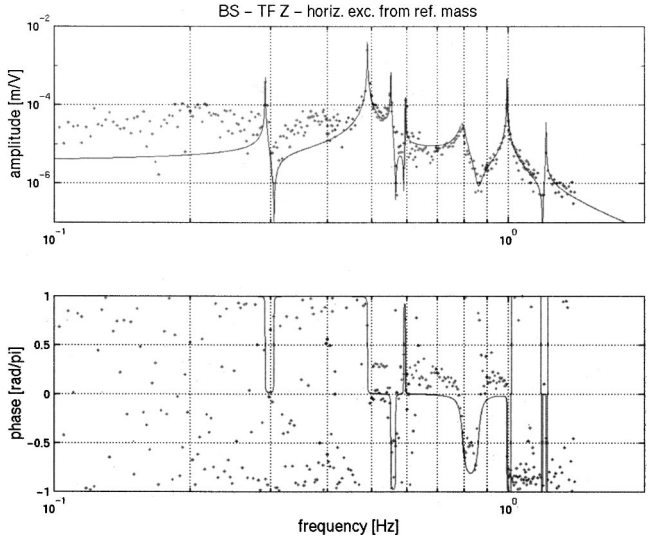


FIG. 5. BS suspension; *Z* transfer function for a force applied on the marionetta with the two horizontal coils of the filter 7 (points) compared with an analytical curve fitted to the data (solid line). In this case the measurement is very noisy below 400 Hz and the only information in low frequency is the position of the mode at 292 mHz.

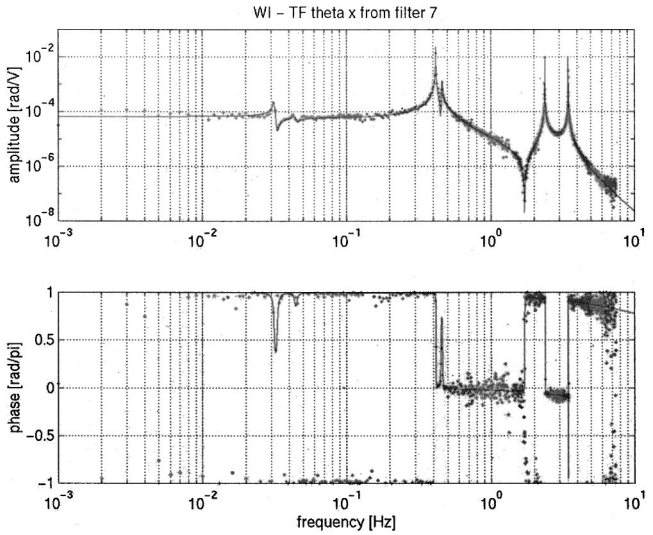


FIG. 7. WI suspension; $\theta x$ transfer function for a torque applied on the marionetta with the two vertical coils of the filter 7 (points) compared with an analytical curve fitted to the data (solid line).

ing BS). At the fiber exit, the reference beam goes to the output (bulk) BS of the interferometer and is split onto two photodiodes. The second exit arm of the FBS is the measurement arm. The beam leaves the fiber through a coupler and polarization control optics and is directed to the test mass through the input window. After the output window there is a second platform supporting a mirror, mounted on a two DOF PZT tilting mount, that is used for fine alignment of the interferometer. The reflected beam goes back to the mirror surface and to the input platform where it is split in two by a beam sampler. The large part of the beam is directed to the output BS of the Mach–Zehnder, where it interferes with the light of the reference arm; the interference fringe pattern is detected by two output photodiodes (PDs). The difference of the two PD signals gives a measure of the changes in the OPL, which in turns depends on the relative displacement of the measurement device and the VIRGO mirror. To obtain a signal proportional to the displacement, the interferometer is locked on the slope of the fringe using the PZT actuator. The actuating signal, that is the signal at the input of the PZT driver, is then proportional to the changes in the OPL difference (provided that the PZT transfer function is flat up to about 100 Hz).

Besides the possibility of making the OPL of the two interferometer arms almost equal (within a few cm, while the measurement arm is more than 6 m long) without increasing the size of the device, the use of fiber optics gives the advantage that the longitudinal actuator (fiber stretcher) is completely decoupled from rotations of the beam, and then we can change the OPL difference by a large amount without affecting the alignment of the interferometer. The main dis-

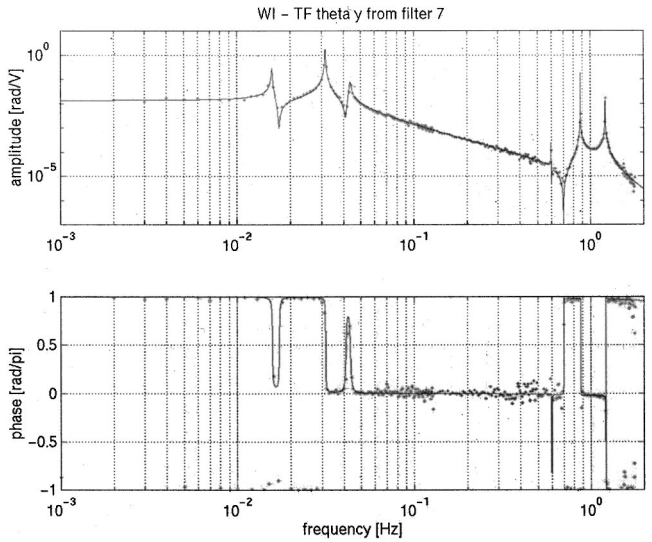


FIG. 6. WI suspension; $\theta y$ transfer function for a torque applied on the marionetta with the two horizontal coils of the filter 7 (points) compared with an analytical curve fitted to the data (solid line).

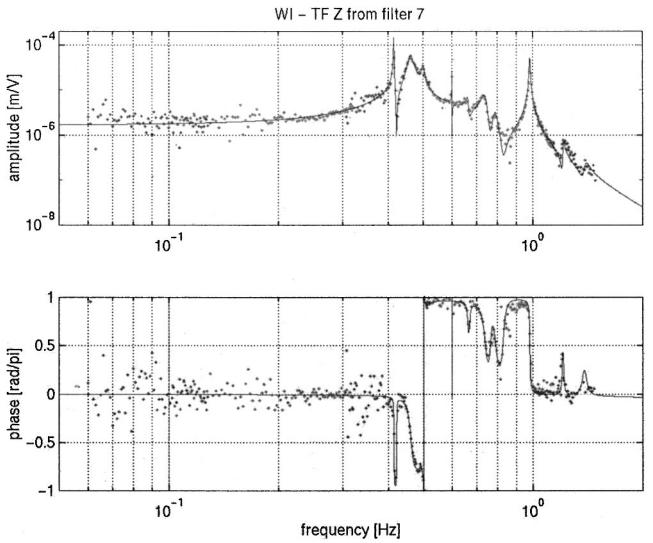


FIG. 8. WI suspension *Z* transfer function for a force applied on the marionetta with the two horizontal coils of the filter 7 (points) compared with an analytical curve fitted to the data (solid line).

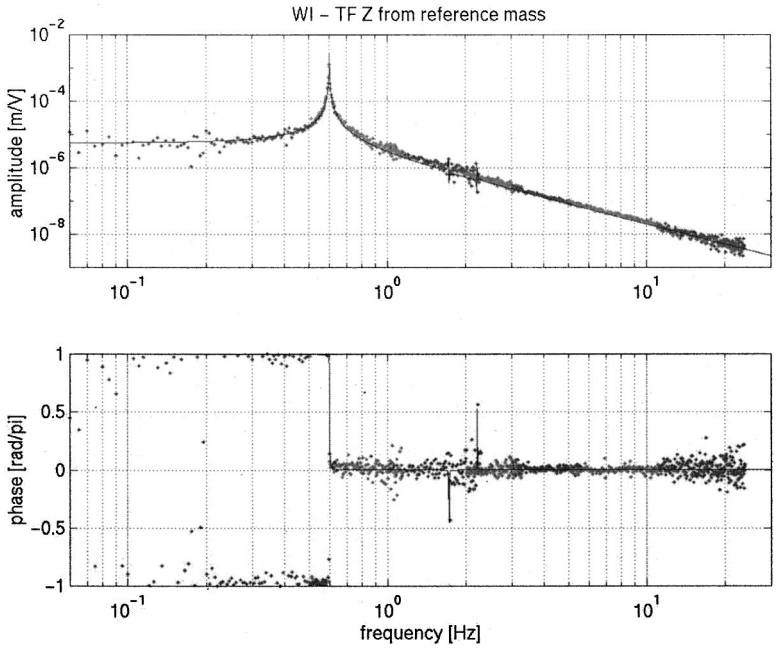


FIG. 9. WI suspension; $Z$ transfer function for a force applied on the mirror with two coils ($U$ and $D$) of the reference mass (points) compared with an analytical curve fitted to the data (solid line).

advantage is that the long fiber (about 4.5 m) becomes sensitive to thermal drifts and acoustic noise.

A smaller fraction of the beam goes on a two-dimensional PSD placed in the focus of a lens; in this way the position of the spot on the sensor only depends on the incidence angle and is almost insensitive (as far as the thin lens approximation holds) to transverse beam displacement.

## III. TRANSFER FUNCTION MEASUREMENTS

The measurement of the transfer functions is performed, with the device described in the previous section, by applying a known signal to the actuators placed on the suspensions and used for the automatic alignment and locking. In particular we are interested in measuring the displacements induced with the four coils attached to the filter 7 legs[6,8] and acting on the marionetta, and with the four coils placed on the reference mass and acting directly on the mirror. At a given frequency, the TF can be measured if the displacement of the mirror induced by the actuators is larger than those the mirror and the measurement device undergo for other causes (mainly seismic noise). Generally we use pairs of actuators (with signals in phase or in counterphase) in order to apply a pure torque or a pure force on the center of mass of the mirror; the cross terms of the TF provide information about the symmetry of the system.

We performed a first TF measurement session to determine the TF of the BS[12] and WI[13] suspensions of the VIRGO central interferometer. In particular, for action on the marionetta from filter 7, the angular ($\theta x$ and $\theta y$) and longitudinal ($Z$) TFs have been measured, in a frequency interval ranging from dc up to a few Hz. For the WI suspension the $Z$ TF has also been measured, from 50 mHz up to ~24 Hz, for forces applied on the mirror from the reference mass. The results are shown in Figs. 3–9. The data are expressed in m/$V$ or rad/$V$ where $V$ is the voltage at the input of the coil drivers; the signal was fed with the same sign (or opposite sign) in the two coils of each pair if we wanted a pure force (or a pure torque, respectively).

Each plot is the result of several measurements, in which the excitation is a pseudorandom (band limited) noise in different frequency bands, with partial overlap; the amplitude is changed according to the mechanical behavior of the system at the different frequencies in order to always obtain a good S/N ratio. The experimental data are compared with an analytical TF, calculated by adjusting frequency and $Q$'s of poles and zeroes to fit the data. The used values, which provide an empirical model of the system, are reported in Tables I–VII; it is worth noting that for the high $Q$ modes we only put a lower limit for the $Q$.

TABLE I. BS suspension; parameters used for the analytical $\theta y$ TF shown in Fig. 3; the dc gain is $10^{-2}$ rad/$V$.

| Poles | | Zeroes | |
|---|---|---|---|
| Freq. (Hz) | $Q$ | Freq. (Hz) | $Q$ |
| 0.014 | 100 | 0.015 | 100 |
| 0.031 | 200 | 0.039 | 50 |
| 0.041 3 | 50 | 0.6536 | $>10^3$ |
| 0.843 75 | $>10^4$ | | |
| 1.193 75 | $>10^4$ | | |

TABLE II. BS suspension; parameters used for the analytical $\theta x$ TF shown in Fig. 4; the dc gain is $10^{-4}$ rad/$V$.

| Poles | | Zeroes | |
|---|---|---|---|
| Freq. (Hz) | $Q$ | Freq. (Hz) | $Q$ |
| 0.4 | 500 | 0.843 | $>10^4$ |
| 0.842 | $>10^4$ | 1.189 5 | $>10^4$ |
| 1.1925 | $>10^4$ | 1.606 25 | 150 |
| 1.635 | 150 | 1.668 75 | 150 |
| 2.25 | $>10^4$ | | |
| 3.42 | $>10^4$ | | |

TABLE III. BS suspension; parameters used for the analytical *Z* TF for action from the filter 7 shown in Fig. 5; the dc gain is $2\times10^{-6}$ m/*V*.

| Poles | | Zeroes | |
|---|---|---|---|
| Freq. (Hz) | *Q* | Freq. (Hz) | *Q* |
| 0.292 | $>10^3$ | 0.3005 | $>10^3$ |
| 0.49 | $>10^3$ | 0.566 | $>10^3$ |
| 0.5525 | $>10^3$ | 0.59 | $>10^3$ |
| 0.595 | $>10^3$ | 0.862 | 50 |
| 0.795 | 40 | 1.19 | $>10^4$ |
| 0.995 | $>10^3$ | | |
| 1.21 | $>10^4$ | | |

## IV. PAYLOAD CONTROL

As explained above, the main motivation for TF measurement, is the characterization of the mechanical behavior of the suspension for forces applied with the actuators used for automatic alignment and locking of the interferometric antenna.

To check that the measurements provide the right information, the measured TFs have been used to design servo-loops that control the position of the test masses, both BS and WI in the three relevant DOF, by using, as error signals, those provided by the TF measurement device itself. The results where satisfactory; in particular we were able for the first time to control the suspension simultaneously with respect to all the three DOF with stable and robust servo-loops. The angular servo-loops were essentially devoted to the damping of the normal modes plus the control of the dc orientation of the mirrors (by the use of an integrator); the control was performed acting on the marionetta through the coils on filter 7.

For the longitudinal control (*Z*), we tested both a normal mode damping acting on the marionetta from filter 7 (BS suspension) and a servo-loop with a larger BW by acting on the mirror from the reference mass (WI suspension). The voltage at the PZT used to control the Mach–Zehnder interferometer of the TF measurement device provided the measurement of the mirror displacement.

For the sake of brevity, we only report the results of the latter servo-loop; in Fig. 10, the open-loop and closed-loop power spectra of the mirror displacement signal are compared; the unity gain of the servo-loop was at about 5 Hz. The control loop was quite stable and worked continuously on the 3 DOF for up to 16 h.

TABLE IV. WI suspension; parameters used for the analytical $\theta y$ TF for action from the filter 7 shown in Fig. 6; the dc gain is $1.32\times10^{-6}$ rad/*V*.

| Poles | | Zeroes | |
|---|---|---|---|
| Freq. (Hz) | *Q* | Freq. (Hz) | *Q* |
| 0.015 75 | 100 | 0.017 25 | 100 |
| 0.0315 | 200 | 0.041 | 50 |
| 0.0435 | 50 | 0.6 | 500 |
| 0.597 | $>10^3$ | 0.7 | $>10^3$ |
| 0.875 | $>10^4$ | | |
| 1.21 | $>10^3$ | | |

TABLE V. WI suspension; parameters used for the analytical $\theta x$ TF for action from the filter 7 shown in Fig. 7; the dc gain is $6.7\times10^{-5}$ rad/*V*.

| Poles | | Zeroes | |
|---|---|---|---|
| Freq. (Hz) | *Q* | Freq. (Hz) | *Q* |
| 0.0314 | 30 | 0.033 | 30 |
| 0.0443 | 20 | 0.0448 | 20 |
| 0.415 | 500 | 0.449 | 100 |
| 0.46 | 100 | 1.7175 | >500 |
| 2.39 | $>10^4$ | | |
| 3.475 | $>10^4$ | | |

TABLE VI. WI suspension; parameters used for the analytical *Z* TF for action from the filter 7 shown in Fig. 8; the dc gain is $1.68\times10^{-6}$ m/*V*.

| Poles | | Zeroes | |
|---|---|---|---|
| Freq. (Hz) | *Q* | Freq. (Hz) | *Q* |
| 0.415 | 400 | 0.422 | 400 |
| 0.462 | 30 | 0.498 | 230 |
| 0.5 | 50 | 0.600 85 | $>10^4$ |
| 0.6 | $>10^4$ | 0.67 | 70 |
| 0.665 | 70 | 0.765 | 50 |
| 0.74 | 30 | 0.83 | 40 |
| 0.789 | 30 | 1.2 | 100 |
| 0.98 | 200 | 1.37 | 40 |
| 1.21 | 100 | | |
| 1.39 | 30 | | |

TABLE VII. WI suspension; parameters used for the analytical *Z* TF for action from the reference mass shown in Fig. 9; the dc gain is $5.6\times10^{-6}$ m/*V*.

| Poles | | Zeroes | |
|---|---|---|---|
| Freq. (Hz) | *Q* | Freq. (Hz) | *Q* |
| 0.600 | >500 | 1.725 | >300 |
| 1.72 | >300 | 2.21 | >500 |
| 2.215 | >500 | | |

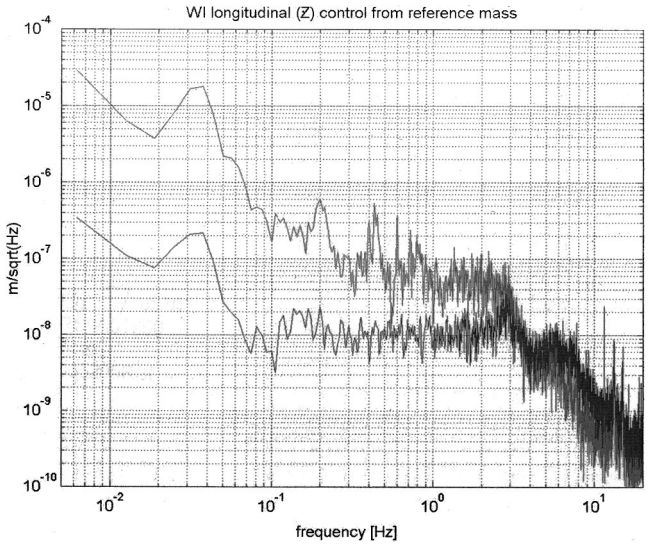


FIG. 10. WI suspension; comparison of open loop (upper line) and closed loop (lower line) *Z* power spectra; FB on mirror from reference mass.

## V. DISCUSSION

In this article we described the device used for the characterization of the last stages of the VIRGO suspensions and report the results of the measurements performed on two on-site suspensions in Cascina. It seems that the general response of the suspensions is in close agreement with the design specifications. Next, we designed the servo-loops for the (local) control of the test mass on three DOF; this is a first step toward the design of the complex servo-loops for the control of the whole antenna. The results are encouraging, since we have shown for the first time the feasibility of the position control of the VIRGO test masses by means of forces internal to the suspension itself only (of course with the exception of dc control, below ~50 mHz, that will be performed on the top stage). The device described in this article permits to obtain useful information for servo-loop design and simulation fine tuning and will be used for the characterization of the other suspensions when necessary. The sensitivity of the measurement is mainly limited by the seismic noise acting on the device itself (this limits the measurement band for forces applied on the marionetta below a few Hz); a substantial improvement can be achieved by the use of vibration isolation platforms for supporting the optical elements of the device. The design already allows the insertion of commercial three-dimensional seismic isolators with resonance frequency around 500 mHz; this will be implemented, if necessary, for the next measurements.

## ACKNOWLEDGMENTS

The authors are grateful to our technicians F. Cassese, B. D'Acquino, M. Di Pietro, M. Favati, G. Pontoriere, R. Rocco, and F. Vignoli for their skillful assistance in the realization and setting up of the device. One of us (L.D.F.) wants to dedicate this work to the memory of Renato Gorini.

[1] For a review about interferometric GW detection see, for example, P. R. Saulson, *Interferometric Gravitational Wave Detectors* (World Scientific, Singapore, 1994).
[2] K. Danzmann in *First Eduardo Amaldi Conference on Gravitational Wave Experiments*, edited by E. Coccia, G. Pizzella, and F. Ronga (World Scientific, Singapore, 1995).
[3] K. Tsubono, in *First Eduardo Amaldi Conference on Gravitational Wave Experiments*, edited by E. Coccia, G. Pizzella, and F. Ronga (World Scientific, Singapore, 1995).
[4] B. Caron *et al.*, Class. Quantum Grav. **14**, 1461 (1997).
[5] P. Fritschel, in *Second Eduardo Amaldi Conference on Gravitational Waves*, edited by E. Coccia, G. Pizzella, and G. Veneziano (World Scientific, Singapore, 1997).
[6] G. Ballardin *et al.*, Rev. Sci. Instrum. **72**, 3643 (2001).
[7] G. Losurdo *et al.*, Rev. Sci. Instrum. **72**, 3653 (2001).
[8] A. Bernardini *et al.*, Rev. Sci. Instrum. **70**, 3463 (1999).
[9] B. Caron *et al.*, Astropart. Phys. **6**, 245 (1997).
[10] M. Barsuglia *et al.*, VIR-NOT-NAP-1390-143, 2000.
[11] E. Calloni *et al.*, Rev. Sci. Instrum. **69**, 1882 (1998).
[12] V. Calbucci *et al.*, VIR-NOT-NAP-1390-173, 2001.
[13] V. Calbucci *et al.*, VIR-NOT-NAP-1390-174, 2001.